

## Structure of the W $L\alpha_{1,2}$ x-ray spectrum

R. Diamant,<sup>1</sup> S. Huotari,<sup>2</sup> K. Hämäläinen,<sup>2</sup> R. Sharon,<sup>1</sup> C. C. Kao,<sup>3</sup> and M. Deutsch<sup>1,\*</sup>

<sup>1</sup>*Physics Department, Bar-Ilan University, Ramat-Gan 52900, Israel*

<sup>2</sup>*Department of Physics, University of Helsinki, P.O. Box 9, FIN-00014 Helsinki, Finland*

<sup>3</sup>*National Synchrotron Light Source, Brookhaven National Laboratory, Upton, New York 11973*

(Received 29 August 2000; published 17 January 2001)

The tungsten  $L\alpha_{1,2}$  x-ray spectrum was measured with high resolution using photoexcitation by monochromatized synchrotron radiation. The line splitting, widths, and relative intensities were determined from a phenomenological fit by five Voigt functions and compared with previous measurements. A fully split diagram and  $5l^{-1}$  spectator hole transition multiplets were calculated *ab initio* using the relativistic multiconfigurational Dirac-Fock method. Fits of various combinations of these multiplets to the measured spectrum show that the line shapes can be well accounted for by the fully split diagram transition  $2p_{3/2}^{-1} \rightarrow 3d_{3/2,5/2}^{-1}$  alone, without invoking contributions from any spectator hole transition.

DOI: 10.1103/PhysRevA.63.022508

PACS number(s): 32.30.Rj, 32.70.-n, 32.80.Fb

### I. INTRODUCTION

The x-ray emission spectra of heavy elements have been less extensively studied than those of low- $Z$  elements. Nevertheless, tungsten enjoyed relatively more attention, perhaps due to its importance as a wavelength standard [1] and its extensive use in applications like radiography and tomography. Most studies, however, concentrated on the excitation cross sections, with focus on the  $L$ -shell Coster-Kronig transitions [2,3], some of which become energetically allowed in this  $Z$  range [4]. The structure of the W  $L$  x-ray spectra was studied by several workers [5–7], most recently by Vlaicu *et al.* [8]. They measured electron-excited  $L\alpha$  and  $L\beta$  spectra and carried out full-spectrum fits to the line shapes using the Dirac-Hartree-Slater (DHS) calculated spectator hole transitions of Parente *et al.* [9]. However, these calculations neglect the coupling of the inner-shell vacancies with the nonfilled outer shells, and consequently do not exhibit the full splitting of the multiplets. Moreover, the relative intensities within each multiplet listed by Parente *et al.* were calculated in the pure  $LS$  coupling. Since the appropriate coupling for the high- $Z$  elements is the almost pure  $jj$  one, those intensities may deviate considerably from the true ones. Thus, we have undertaken a study of the  $L\alpha_{1,2}$  spectrum using photoexcitation by monochromatized synchrotron radiation, and recording the emitted radiation by a high-resolution Johann-type crystal spectrometer. The values of the various quantities derived directly from the measured spectrum are listed and compared with previous measurements and show a reasonable overall agreement. *Ab initio* relativistic multiconfigurational Dirac-Fock calculations were employed to obtain fully split multiplets of the relevant diagram and spectator hole transitions. These were fitted to the measured data to elucidate the underlying structure of the  $L\alpha_{1,2}$  spectrum. The fits demonstrate that the line shapes can be satisfactorily accounted for by the diagram transitions only, and there is no need to invoke contributions from spectator hole transitions. Further measurements and calculations

indicated by the present results are also discussed.

### II. EXPERIMENT AND ANALYSIS

The measurements were done using synchrotron radiation at the X25 wiggler beam line, NSLS, Brookhaven National Laboratory. The monochromatized incident flux at the 50- $\mu\text{m}$ -thick W foil sample was  $\sim 10^{12}$  photons/sec in a spot  $\sim 1$  mm wide. The emission spectra were recorded with a Johann-type spectrometer using a spherically bent Si(444) analyzer. The  $\sim 72^\circ$  Bragg angle provided a resolution of 2.8 eV [10,11]. The measured spectra were corrected for (i) the time variation of the monochromatic incident beam intensity, which was monitored by an ion chamber, (ii) the absorption in the sample of both incident and emitted radiation, and (iii) the dead time of the electronics and multichannel analyzer used for pulse height discrimination of signals. Further details on the experimental setup are given elsewhere [12–14].

The *ab initio* calculations employed the relativistic multiconfigurational Dirac-Fock (RMCDF) code GRASP [15]. Previous studies [16,17] indicate the importance of allowing in the calculations a full relaxation of the excited atom prior to the emission process. This is done by generating in all cases the initial- and final-state wave functions in separate, independent runs. The energies of the individual transitions are then obtained by subtracting the energies of the appropriate level, as calculated in the initial- and in the final-state runs. However, these separate runs resulted in the initial- and final-state wave functions being nonorthogonal, which, in turn, did not allow their simultaneous use in the relative transition probability calculations. Thus, as in previous studies [12,14,16,18], configuration interaction calculations were carried out to obtain the various transition probabilities using once the initial-state orbitals and again the final-state orbitals. As in previous cases, all significant transition probabilities in the two sets agreed closely with each other. The calculations addressed both the single-electron diagram spectrum  $2p_{3/2} \rightarrow 3d_{3/2,5/2}$  (underlining denotes hole states) and the spectator hole transitions  $2p_{3/2}nl \rightarrow 3d_{3/2,5/2}nl$  with  $nl = 4p, 5s, 5p, 5d, \text{ and } 6s$ . The results are discussed in the next section.

\*Corresponding author. Email: deutsch@mail.biu.ac.il

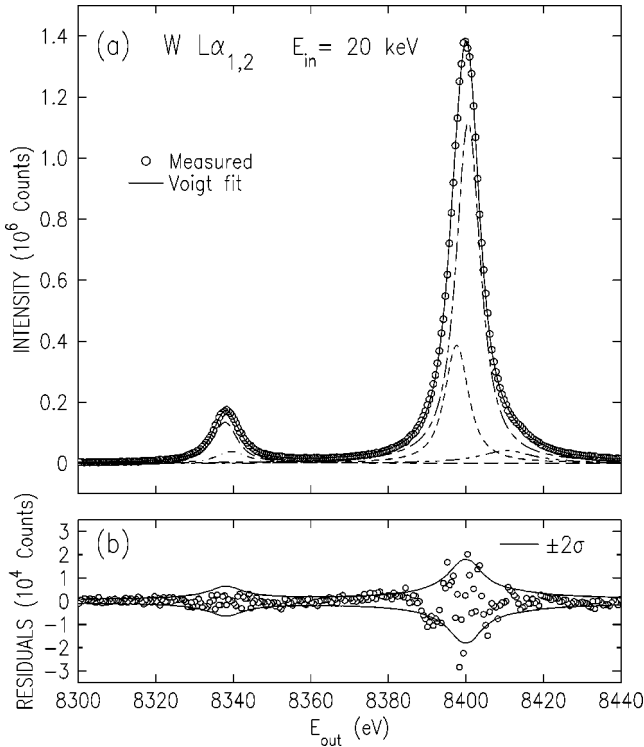


FIG. 1. (a) The measured  $W L\alpha_{1,2}$  spectrum (points) with a phenomenological fit to a sum of five Voigt functions (lines). (b) The fit residuals. The good fit is indicated by the residuals being almost all within the  $\pm 2\sigma$  boundaries of the measured values, where  $\sigma$  is the standard deviations in the measured values.

### III. RESULTS AND DISCUSSION

#### A. Spectral characteristics

The measured  $W L\alpha$  spectrum for an incident photon energy of  $E_{in}=20$  keV is shown in Fig. 1(a), along with a phenomenological fit to a sum of Voigt functions. Such a sum provides in general a representation of measured emission lines superior to that of sums of Lorentzians or Gaussians [8,12,16,18]. The Gaussian component of the Voigt function represents the spectrometer's resolution function while the Lorentzian component represents the true shape of a single emission line. The Gaussian width was kept fixed in the fit at the resolution value of 2.8 eV, as discussed above, and the widths, amplitudes, and positions of the Lorentzian components of the Voigt functions were refined. The minimal number of Voigt functions required for a good fit to the data was found to be three for  $L\alpha_1$  and two for  $L\alpha_2$ . The highest-energy Voigt function, centered on  $\sim 8414$  eV, is required to fit the  $L\alpha'$  satellite [19] on the high-energy tail of the  $L\alpha_1$  line. Discounting this feature, two Voigt functions are still required to fit each of the two spectral lines. The fact that a single Voigt function for each line is insufficient indicates underlying structure, the origin of which is discussed in Sec. III B. The good quality of the fit obtained with these five Voigt functions is demonstrated in Fig. 1(b), where almost all residuals are bounded by the  $\pm 2\sigma$  lines ( $\sigma$  is the standard deviation of each data point due to the counting statistics). Note also the vanishingly low background in our

TABLE I. Comparison of the values obtained from the fit in Fig. 1 ("Present") with previous theoretical and experimental values. The  $\Gamma$ 's are the full widths at half maximum of the two lines as derived from Voigt function fits. The numbers in parentheses are the uncertainties in the last digit of the respective values.

Source	Widths		Splitting $\Delta E_{L\alpha_1-L\alpha_2}$ (eV)	Ratio $I(L\alpha_2)/I(L\alpha_1)$ (%)
	$\Gamma_{L\alpha_1}$ (eV)	$\Gamma_{L\alpha_2}$ (eV)		
Experiment				
Present	7.8(4)	7.4(4)	62.2(1)	11.6(3)
SL <sup>a</sup>	7.9(6)	5.3(5)		11.2
GSS <sup>b</sup>	6.6(3)	6.7(4)	62.0	
Vea <sup>c</sup>	7.0(5)	7.3(1)		11.4(1) <sup>d</sup> 11.4(1) <sup>e</sup>
BB <sup>f</sup>			62.4(4)	
Theory				
Present: diagram			62.2 <sup>g</sup>	12.0 <sup>g</sup>
<u>5d</u> spect.			62.3 <sup>g</sup>	10.8 <sup>g</sup>
M <sup>h</sup>	6.45	7.86		
Cea <sup>i</sup>	6.64	6.68		
Vea <sup>c</sup>	6.607	6.68		
S <sup>j</sup>				11.34
Pea <sup>k</sup>	6.32	7.13	64.90	11.33

<sup>a</sup>Salem and Lee, Ref. [20].

<sup>b</sup>Gokhale, Shukla, and Srivastava, Ref. [7].

<sup>c</sup>Vlaicu *et al.*, Ref. [8].

<sup>d</sup>Calculated multiplets' fit using Voigt functions.

<sup>e</sup>Phenomenological fit using Voigt functions.

<sup>f</sup>Bearden and Burr, Ref. [23].

<sup>g</sup>From our relativistic Dirac-Fock calculations. See text.

<sup>h</sup>McGuire, Ref. [24]. See also Table II in Gokhale *et al.*, Ref. [7].

<sup>i</sup>Using  $\Gamma(L_3)$  of Chen *et al.*, Ref. [25] and  $\Gamma(M_i)$  of Chen *et al.*, Ref. [26].

<sup>j</sup>Scofield, Ref. [27].

<sup>k</sup>Perkins *et al.*, Ref. [21].

photon-excited spectrum in Fig. 1 (a), as compared to electron excited spectra, e.g., Fig. 1 in [7] and Fig. 1 in [8]. This is due to the total absence of bremsstrahlung, the main background contribution in electron-excited spectra.

The five-Voigt fit was employed to derive quantitative values for the various characteristics of the  $W L\alpha_{1,2}$  spectrum. These are given in the first line of Table I, which also lists previous experimental and theoretical values. The theoretical values denoted "Present" were obtained from the *ab initio* RMCDF-calculated multiplet spectra, as discussed below. As observed in the table, our measurements yield  $\Gamma_{L\alpha_1} \approx \Gamma_{L\alpha_2}$  within the combined experimental uncertainties. This agrees with all previous experimental results except that of Salem and Lee [20]. While their  $\Gamma_{L\alpha_1}$  is in good agreement with ours, their  $\Gamma_{L\alpha_2}$  is anomalously low in comparison with both their  $\Gamma_{L\alpha_1}$  and all other measured and calculated  $\Gamma_{L\alpha_2}$ . The photographic study of Gokhale *et al.* [7] yields systematically lower widths for both lines as compared to ours and Vlaicu *et al.* [8]. Our widths agree, however, with

the recent detailed study of Vlaicu *et al.* to within the combined uncertainties. The agreement is even better when one considers that Vlaicu *et al.* use a *single* Voigt function to represent each of the two spectral lines, while we use several, as discussed above. Using a single Voigt function to fit each line of our data yields  $\Gamma_{L\alpha_1} = 6.9$  eV and  $\Gamma_{L\alpha_2} = 7.4$  eV, very close to the results of Vlaicu *et al.* However, the quality of the fit deteriorates from a  $\chi^2 = 1.9$  obtained for the five-Voigt fit shown in Fig. 1 and listed in Table I to  $\chi^2 = 8.8$  for a two-Voigt fit, similar to that of Valicu *et al.* Thus, based on the  $\chi^2$ , our five-Voigt fit and the resultant spectral quantities provide a better description of the line shapes. However, the differences between the experimental values of Vlaicu *et al.* and ours are smaller than those between experiment and the more recent theoretical values. This may result either from overlooking some contributions to the level widths in the theoretical calculation, or from having contributions to the lines, additional to those of the diagram transitions, which broaden the measured line. This point will be further discussed in Sec. III B. The  $\Gamma$  values of Perkins *et al.* [21] deviate from the rest of the results. These Dirac-Hartree-Slater calculations are known to overestimate the strength of Coster-Kronig transitions [21]. Although corrections were applied, the claimed accuracy for the Auger widths is no better than 15%, and can reach a factor of 2, while the radiative width is accurate to  $\sim 10\%$  [21]. With these accuracies the disagreement between the experimental linewidths and those based on the values of Perkins *et al.* is not too severe, although the results of both Vlaicu *et al.* and us do not seem to support the  $\sim 0.8$ -eV difference in the widths of the two lines, emerging from the calculations of Perkins *et al.*

The splitting of the two lines agrees well with both previous experimental and theoretical results, except for that of Perkins *et al.* [21], who overestimate the measured splitting by  $\approx 2.5$  eV. All theoretical and experimental values of the intensity ratio of the two lines, including ours, agree to within  $\sim 0.3\%$ . The theoretical values derived from our RM-CDF calculations seem to deviate by slightly more than that, although the discrepancy is a mere  $\sim 5\%$ .

Finally, we have measured the W  $L\alpha_{1,2}$  spectrum excited with incident photons of energies ranging from 17.5 to 23.5 keV, in steps of 1 keV, to detect possible changes in the line shapes. After application of the corrections discussed above all measured spectra were found to be identical and yielded coinciding values for the quantities listed in Table I.

### B. Comparison with theory

The five-Voigt fit discussed above indicates an underlying structure in the spectral lines. One possibility for the origin of this structure are spectator transitions, i.e., transitions identical to the diagram one but in the presence of one or more (inner shell) holes created along with the main  $2p_{3/2}$  vacancy in which the diagram transition originates. Such spectator transitions were identified as significant contributors to the line shape of  $3d$  transition elements [16,18]. A second possibility is that the diagram transition, when fully split due to the coupling of the inner-shell vacancies with the

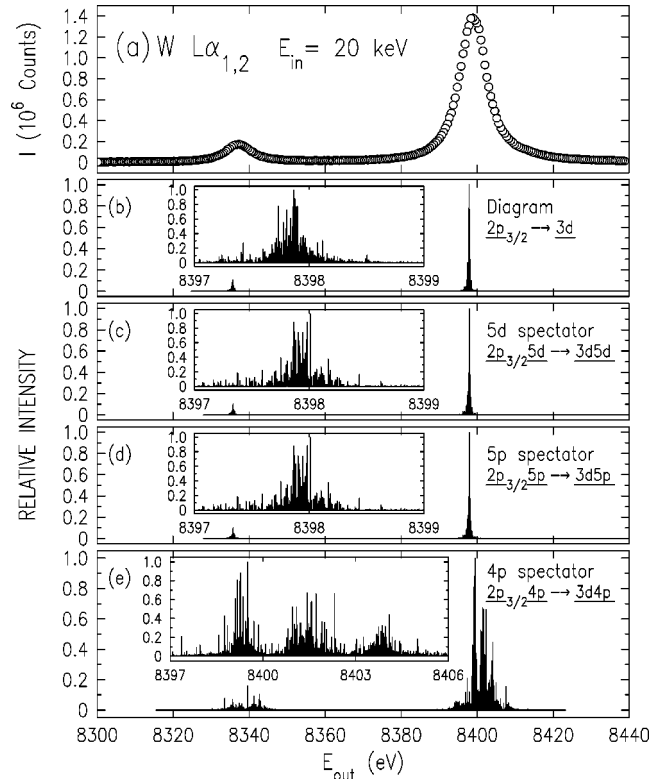


FIG. 2. (a) The measured W  $L\alpha_{1,2}$  spectrum. (b)–(e) The RM-CDF-calculated spectra of the diagram and indicated spectator hole transitions. The insets show the  $L\alpha_1$  region on a magnified scale. Note that only the  $4p$  spectator hole multiplet is shifted and split by a significant amount and all higher-shell spectator hole multiplets appear to be very similar to the diagram multiplet.

outer, semifilled shells, is responsible for the structure underlying the spectrum. Vlaicu *et al.* [8] studied the first of these possibilities. However, they did not employ fully split calculated multiplets for either the diagram or the spectator transitions. Instead, they used the Dirac-Hartree-Slater (DHS) calculations of Parente *et al.* [9], which neglect the coupling of the inner-shell vacancies to the semifilled outer shells, as well as the electron-electron Coulomb correlations. Moreover, the relative line intensities within each multiplet in that calculation are valid only in the pure  $LS$  coupling limit, i.e., for low- $Z$  elements. By contrast, the high- $Z$  tungsten obeys the  $jj$  coupling scheme. The DHS calculations should yield energies as accurate as fully split relativistic Dirac-Fock calculations, albeit with much fewer lines. However, the  $LS$ -limit relative intensities cannot be expected to be reliable for tungsten. This, and the potential importance to the line shape of fully split multiplets prompted us to adopt a different approach.

We have carried out fully split *ab initio* RM-CDF calculations for the diagram W  $L\alpha_{1,2}$  transition,  $2p_{3/2} \rightarrow 3d_{3/2,5/2}$ , as well as several single spectator transitions  $2p_{3/2}nl \rightarrow 3d_{3/2,5/2}nl$ . Earlier studies [16,18] indicate that the outer, weakly bound electrons are most likely to be shaken off along with the direct ionization of the initial hole and thus the corresponding vacancies are the most likely to be the spectators during the subsequent transition. For example, in

TABLE II. Fit results for different combinations of the RMCDF-calculated diagram and  $5d$  spectator hole multiplets to the measured data for (a)  $2p_{3/2} \rightarrow 3d$  transitions only, (b)  $1s \rightarrow 2p_{3/2} + 2p_{3/2}5d \rightarrow 3d5d$ . The calculated intensity ratio of the  $L\alpha_1$  and  $L\alpha_2$  line groups was constrained to the calculated values for both (a) and (b). (c) and (d) are the corresponding fits to (a) and (b) but without constraints on the relative intensities.  $I_{int}$  is the integrated intensity relative to that of the full spectrum.

Parameter	Vacancy	Unit	(a)	(b)	(c)	(d)
Shift	$3d$	eV	2.2	2.9	2.2	2.9
	$3d5d$			0.6		0.6
Width	$3d_{5/2}$	eV	7.2	7.6	7.2	7.5
	$3d_{3/2}$		7.0	6.2	6.8	6.8
	$3d_{5/2}5d$			5.4		5.6 <sup>a</sup>
	$3d_{3/2}5d$			8.2		5.6 <sup>a</sup>
Intensity	$3d_{5/2}$	%	100	100	100	100
	$3d_{3/2}$				101	130
	$3d_{5/2}5d$			63		89
	$3d_{3/2}5d$					41
$I_{int}$	$3d_{5/2}$	%	89.3	54.8	89.4	63.6
	$3d_{3/2}$		10.7	6.6	10.6	9.0
	$3d_{5/2}5d$			34.9		26.1
	$3d_{3/2}5d$			3.7		1.3
$\chi^2$			8.0	5.0	7.6	4.7

<sup>a</sup>These two widths were constrained to be equal in the fit.

Cu, whose outermost occupied shell is  $4s$ , the  $3d$  spectator hole transition  $1s3d \rightarrow 2p3d$  was found [16] to contribute about 27% to the spectral intensity, while the more inner  $3p$  spectator transition  $1s3p \rightarrow 2p3p$  contributes only  $\leq 0.5\%$ . Guided by these findings, we have calculated for W, whose outermost occupied shell is  $6s$ , spectator multiplets for  $nl = 6s$ ,  $5d$ , and  $5p$ . The  $4p$  spectator multiplet was also calculated to gain insight into the evolution of the multiplets' positions and splitting for progressively inner vacancies.

The calculated diagram and spectator multiplets (except for the  $6s$ , which is identical with the diagram multiplet) are shown in Fig. 2. The general appearance, the splitting between the two main groups of lines, and the relative intensities, are faithfully reproduced for all  $5l$  spectators and the diagram multiplet, albeit with a consistent  $\sim 1$ -eV downshift relative to the experiment. Such small shifts between the calculated and measured spectra were noted by several authors, and are within the expected accuracy of the calculations. The insets show, however, that progressing from the outermost shell in, the spectators cause an increasing splitting within each of the two main line groups. The  $4p$  spectator [Fig. 2(e)] shows an extended group of intense lines, spread over  $\sim 8$  eV and upshifted by 4–5 eV relative to the diagram multiplet in Fig. 2(b). This puts a considerable portion of their lines outside the width of the measured lines. Thus, the calculated multiplets indicate that only  $5l$  spectators are likely to contribute significantly to the  $L\alpha_{1,2}$  line shapes. We have, therefore, carried out fits of the measured spectrum to sums of multiplets in several combinations using a previously developed method [8,16,18].

The fits were carried out in several stages, concentrating on the diagram and the  $5d$  spectator multiplets. First, only

the diagram multiplet was fitted, with the intensity of the  $5d$  spectator spectrum set to zero, and the intensity ratio between the  $L\alpha_1$  and  $L\alpha_2$  lines kept at the calculated value. At this stage only two linewidths, each common to all  $L\alpha_1$  or all  $L\alpha_2$  lines (respectively) of the multiplet, a single shift, and an overall intensity were refined in the fit. The resultant parameters are denoted by (a) in Table II. In fit (b) a sum of the diagram and the  $5d$  spectator multiplets was fitted, refining for each the same (but independent) set of parameters as in (a). Fits (c) and (d) correspond to (a) and (b), respectively, but the restriction on keeping the relative intensity of the  $L\alpha_1$  and  $L\alpha_2$  line groups at the calculated value was removed and two intensities were refined for each multiplet: one each for lines of the  $L\alpha_1$  and the  $L\alpha_2$  groups. Fit (b), its residual, and the residual of fit (a) are plotted in Fig. 3. The parameters obtained in all fits are listed in Table II.

As seen in Fig. 3(a), fit (b), which employs both the diagram and the  $5d$  spectator multiplets, yields a reasonable agreement with the measured spectrum. Most residuals in Fig. 3(b) (open circles), though not all, are bound by  $\pm 3\sigma$ . The residuals are, however, almost identical with those of fit (a) (solid circles), which employs only the diagram multiplet. The  $\sim 27\%$  reduction in  $\chi^2$  upon including the  $5d$  multiplet in the fit is due only to a slight improvement in the fit near the peaks, where the intensity is high. Moreover, we find that it is possible to obtain fits with a significantly lower intensity for the  $5d$  spectator multiplet, with only a small, 5–10%, increase in  $\chi^2$  relative to that of fit (b). Removing the constraint of keeping the relative intensity of the  $L\alpha_1$  and  $L\alpha_2$  groups at the calculated value, for both the diagram and  $5d$  spectator multiplets makes only a small change in the fits, as can be observed by comparing columns (a) and (b) with (c)

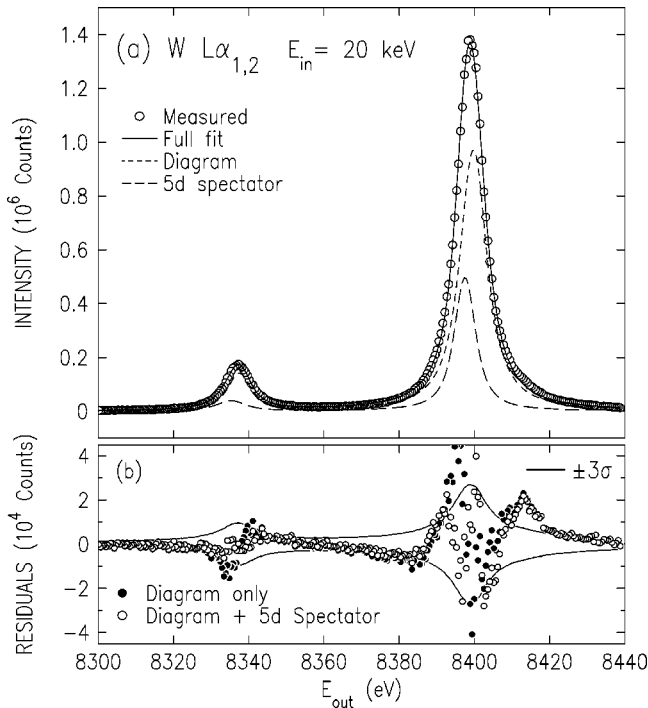


FIG. 3. The measured (points) and the fitted (lines) RMCDF theoretical spectrum of fit (b) in Table II. (b) The fit residuals. The inclusion of the  $5d$  spectator hole multiplet improves the fit only marginally. The small peak at  $\sim 8414$  eV in (b) is due to the  $L\alpha'$  satellite.

and (d), respectively, in Table II. The integrated intensities,  $I_{int}$ , of the various lines hardly change, and the reduction in  $\chi^2$  is only  $\sim 5\%$ . Thus, although the creation of  $5d$  spectator holes along with the direct ionization of the  $2p_{3/2}$  electron is highly likely, and consequently a significant contribution of the corresponding spectator transition to the line shape is also highly likely, a clear separation of such a contribution from that of the diagram is not possible. This is in contrast with Cu [16] and Sc [18], where such separation was possible. This difference stems from the levels involved being considerably different. Thus, the linewidth of W is threefold larger than that of Cu and Sc, effectively masking the relatively small,  $\lesssim 1$  eV additional splitting and shift due to the spectator hole. It may be possible to separate out the spectator contribution in coincidence measurements on the emitted electrons when the initial state is created, or by carefully measuring the differences in the line shape near the  $2p_{3/2}5d$  excitation threshold, where below the edge only the diagram, and above it both diagram and spectator transition should be

excited. However, until such evidence is presented, and since the diagram-only fit is just marginally worse than the diagram-plus-spectator one, Occam's Razor [22] leads to the conclusion that the  $L\alpha_{1,2}$  spectrum stems from the diagram transition only, its underlying structure is determined by the structure of the fully split diagram multiplet, and the contribution to the line shape from satellites due to spectator hole transitions is negligible. This conclusion agrees with Vlaicu *et al.*, who find a contribution of  $\lesssim 5\%$  from spectator transitions to the line shape.

Finally, all fits reveal a localized peak centered at  $\sim 8414$  eV in Fig. 3(b). This is the  $L\alpha'$  satellite, which originates in a  $3l$  spectator hole transition, and the exact assignment of which is discussed elsewhere [19]. In addition, extended deviations can be observed in the residuals in Fig. 3(b) on both sides of the two peaks. While rather small, these deviations are systematic, and deserve further study. One likely source for them may be Coster-Kronig satellites, as pointed out by Vlaicu *et al.* [8]. Measurements of the  $L\alpha_{1,2}$  line shape variation with the exciting radiation's energy as it is varied across the  $L_1$ ,  $L_2$ , and  $L_3$  edges should, in principle, allow a quantitative assessment of the contribution of Coster-Kronig transitions to the W  $L\alpha_{1,2}$  spectrum's shape and intensity.

#### IV. CONCLUSIONS

The high-resolution study of the W  $L\alpha_{1,2}$  spectrum presented here provides an accurate determination of the line shapes, as well as the various quantities derived therefrom: widths, splitting, and relative intensity. A phenomenological representation by a five-Voigt function fit indicates a highly overlapping underlying structure within the lines. Fits of the measured spectrum to sums of fully split *ab initio* RMCDF-calculated multiplets lead to the conclusion that the structure apparent in these lines is due to the diagram transition only, and no significant contributions to the line shapes from spectator hole transitions can be supported by the measurements. Small but systematic deviations in the fit residuals hint at other contributions, possibly from Coster-Kronig transitions, indicating the need for further, excitation-energy-dependent measurements across the  $L$  edges of tungsten.

#### ACKNOWLEDGMENTS

Partial support by the Israel Science Foundation, Jerusalem (M.D.) and the Academy of Finland under Grants No. 7379 and 40732 (K.H. and S.H.), and beamtime at X25, NSLS, are gratefully acknowledged. Brookhaven National Laboratory is supported by the U.S. DOE under Contract No. DE-AC02-76CH00016.

- [1] E. G. Kessler, Jr., A. Henins, and R. D. Deslattes, Phys. Rev. A **19**, 215 (1979); R. D. Deslattes, A. Henins, and E. G. Kessler, Jr., Ann. Phys. (N.Y.) **129**, 378 (1980).
- [2] U. Werner and W. Jitschin, Phys. Rev. A **38**, 4009 (1988).
- [3] R. Durak and Y. Özdemir, J. Phys. B **31**, 3575 (1998); M. Şahin, L. Demir, M. Ertuğrul, and O. İçelli, *ibid.* **33**, 93 (2000), and references therein.

- [4] T. Papp, J. L. Campbell, and S. Raman, Phys. Rev. A **49**, 729 (1994); W. Jitschin, R. Stotzel, T. Papp, M. Sarkar, and G. D. Dolen, *ibid.* **52**, 977 (1995); T. Papp, J. L. Campbell, and D. Varga, in *Proceedings of the 17th International Conference on X-Ray and Inner-Shell Processes, Hamburg, Germany*, edited by R. L. Johnson, H. Schmidt-Böcking, and B. F. Sonntag,

- AIP Conference Proceedings No. 389 (AIP, New York, 1997), p. 431.
- [5] A. N. Nigam, R. B. Mathur, and R. Jain, *J. Phys. B* **18**, 2489 (1974).
- [6] L. Salguero, M. L. Carvalho, and F. Parente, *J. Phys. (Paris), Colloq.* **48**, C9-609 (1987).
- [7] B. G. Gokhale, S. N. Shukla, and R. N. Srivastava, *Phys. Rev. A* **28**, 858 (1983).
- [8] A. M. Vlaicu, T. Tochio, T. Ishizuka, D. Ohsawa, Y. Ito, T. Mukoyama, A. Nisawa, T. Shoji, and S. Yoshikado, *Phys. Rev. A* **58**, 3544 (1998).
- [9] F. Parente, M. H. Chen, B. Crasemann, and H. Mark, *At. Data Nucl. Data Tables* **26**, 383 (1981).
- [10] With a width of  $w \approx 1$  mm for the incident beam's focus at the sample, an analyzer/sample distance of  $L=95$  cm, an energy  $E=8330$  eV, and a Bragg angle of  $\theta_B=72^\circ$  the calculated resolution [11]  $\delta E = Ew/(L \tan \theta_B) = 2.8$  eV. The same value was obtained employing a ray tracing program for the experimental setup, from the source to the detector.
- [11] K. Hämäläinen, D. P. Siddons, J. B. Hastings, and L. E. Berman, *Phys. Rev. Lett.* **67**, 2850 (1991); C. C. Kao, W. A. Caliebe, J. B. Hastings, K. Hämäläinen, and M. H. Krisch, *Rev. Sci. Instrum.* **67**, 1 (1996); K. Hämäläinen, M. Krisch, C. C. Kao, W. Caliebe, and J. B. Hastings, *ibid.* **66**, 1699 (1995).
- [12] M. Deutsch, O. Gang, K. Hämäläinen and C. C. Kao, *Phys. Rev. Lett.* **76**, 2424 (1996); M. Fritsch, C. C. Kao, K. Hämäläinen, O. Gang, E. Förster, and M. Deutsch, *Phys. Rev. A* **57**, 1686 (1998).
- [13] R. Diamant, S. Huotari, K. Hämäläinen, C. C. Kao, and M. Deutsch, *Phys. Rev. Lett.* **84**, 3278 (2000).
- [14] R. Diamant, S. Huotari, K. Hämäläinen, C. C. Kao, and M. Deutsch, *Phys. Rev. A* **62**, 052519 (2000).
- [15] K. G. Dyall, I. P. Grant, C. T. Johnson, F. A. Parpia, and E. P. Plummer, *Comput. Phys. Commun.* **55**, 425 (1989).
- [16] M. Deutsch, G. Hölzer, J. Härtwig, J. Wolf, M. Fritsch, and E. Förster, *Phys. Rev. A* **51**, 283 (1995).
- [17] J. W. Cooper, *Phys. Rev. A* **38**, 3417 (1988); H. P. Saha, *ibid.* **42**, 6507 (1990); M. H. Chen, in *Atomic Inner Shell Physics*, edited by B. Crasemann (Plenum, New York, 1986).
- [18] D. F. Anagnostopoulos, R. Sharon, D. Gotta, and M. Deutsch, *Phys. Rev. A* **60**, 2018 (1999).
- [19] R. Diamant, S. Huotari, K. Hämäläinen, R. Sharon, C. C. Kao, and M. Deutsch, *J. Phys. B* **33** L649 (2000).
- [20] S. I. Salem and P. L. Lee, *Phys. Rev. A* **10**, 2033 (1974).
- [21] S. T. Perkins, D. E. Cullen, M. H. Chen, J. H. Hubbell, J. Rathkopf, and J. Scofield, Lawrence Livermore National Laboratory Report No. UCRL-50400, 1991 (unpublished), Vol. 30. See also M. Deutsch, O. Gang, G. Hölzer, J. Härtwig, J. Wolf, M. Fritsch, and E. E. Förster, *Phys. Rev. A* **52**, 3661 (1995).
- [22] M. Wildner, *Lancet* **354**, 2172 (1999); J. Greenwood, *Nature (London)* **324**, 21 (1986); G. I. Webb, *J. Artif. Intell. Res.* **4**, 397 (1996).
- [23] J. A. Bearden and A. F. Burr, *Rev. Mod. Phys.* **39**, 125 (1967).
- [24] E. J. McGuire, *Phys. Rev. A* **5**, 1043 (1972).
- [25] M. H. Chen, B. Crasemann, and H. Mark, *Phys. Rev. A* **24**, 177 (1981).
- [26] M. H. Chen, B. Crasemann, and H. Mark, *Phys. Rev. A* **21**, 449 (1980).
- [27] J. H. Scofield, *At. Data Nucl. Data Tables* **14**, 121 (1974).